**Thomas J. Bruno**[1]
**Lisa S. Ott**[1]
**Tara M. Lovestead**[1]
**Marcia L. Huber**[1]

[1] Thermophysical Properties Division, National Institute of Standards and Technology, Boulder, USA.

Review

# Relating Complex Fluid Composition and Thermophysical Properties with the Advanced Distillation Curve Approach*

Complex fluids have long posed a significant challenge in our ability to characterize and model fluid properties. Here, complex fluids are considered to be mixtures with many components that can differ significantly in polarity and polarizability. The penultimate complex fluid is crude oil, although many other fluids such as finished fuels are also highly complex. We have recently introduced a measurement strategy that can simplify these efforts and provides the added potential of linking chemical composition (i.e. analytical) information with physical property information. In addition to chemical characterization, the approach provides the ability to calculate thermodynamic and transport properties for such complex heterogeneous streams. The technique is based on the advanced distillation curve (ADC) metrology, which separates a complex fluid by distillation into fractions that are sampled, and for which thermodynamically consistent temperatures are measured at atmospheric pressure. The collected sample fractions can be analyzed by any method that is appropriate. Analytical methods we have applied include gas chromatography (with flame ionization, mass spectrometric and sulfur chemiluminescence detection), thin-layer chromatography, FTIR, Karl Fischer coulombic titrimetry, refractometry, corrosivity analysis, neutron activation analysis and cold neutron prompt gamma activation analysis. This method has been on product streams such as finished fuels (gasoline, diesel fuels, aviation fuels, rocket propellants), crude oils (including a crude oil made from swine manure) and waste oil streams (used automotive and transformer oils). In this review, we describe the essential features of the ADC metrology with illustrative examples.

**Keywords:** Chemical analysis, Distillation curve, Equation of state, Petroleomics

*Received:* November 24, 2009; *accepted:* January 05, 2010

**DOI:** 10.1002/ceat.200900562

## 1 Introduction

The analysis of complex fluids such as crude oils, fuels, vegetable oils and mixed waste streams has posed significant challenges arising primarily from the multiplicity of components, the different properties of the components (polarity, polarizability, etc.) and matrix properties (such as dirty samples). Indeed, the new field of petroleomics is geared to provide a detailed understanding of such fluids, especially those derived from fossil feedstocks [1]. The term petroleomics was first coined by Marshall and Rodgers, describing the application of ultrahigh resolution mass spectrometry to such complex fluids as crude oils [2]. Petroleomics, according to these authors, is the "relationship between the chemical composition of a fossil fuel and its properties and reactivity". Indeed, in recent years, many analytical methods have been applied to crude oils, the finished fuels derived from them, and the waste products generated in the course of using them [3]. These include nearly all types of gas, liquid and supercritical fluid chromatography, coupled with nearly all types of detectors and sampling methods. Moreover, nearly every spectroscopic method has been

**Correspondence:** Dr. T. Bruno (bruno@boulder.nist.gov), Thermophysical Properties Division, National Institute of Standards and Technology, MS 838.00, 325 Broadway, Boulder, CO 80305, USA.



  

applied as well. The application of ultrahigh-resolution mass spectroscopic techniques, such as Fourier transform ion cyclotron resonance, is perhaps at the pinnacle of analytical techniques applied to such complex fluids [2]. Current limitations in the advancement of petroleomics, as asserted by Marshall and Rodgers, include quantitation of species, modeling and informatics. Indeed, most of the strikingly successful work has been in very detailed compound identification. The difficulty lies in establishing the relationship between the chemical composition and the properties of the fluid, specifically the physical properties. This difficulty results from the intermolecular interactions that occur among species present in a complex fluid such as a crude oil or even a finished fuel. Thus, fundamental physical properties (thermodynamic and transport properties) have not been easily obtainable from a composition suite, however detailed.

One of the most important and informative properties that is measured for complex fluid mixtures is the distillation (or boiling) curve [4, 5]. Simply stated, the distillation curve is a graphical depiction of the boiling temperature (at atmospheric pressure) of a fluid or fluid mixture plotted against the volume fraction distilled. The distillation curve provides the only practical avenue to assess the vapor liquid equilibrium (volatility) of a complex mixture. The standard test method, ASTM D-86, provides the classical approach to measurement, yielding the temperature at predetermined distillate volume fractions and the final boiling point [6]. The ASTM D-86 test suffers from several drawbacks, including large uncertainties in temperature measurements and little theoretical significance. We recently introduced an improved method, called the composition-explicit or advanced distillation curve (ADC) [7, 8]. The ADC approach addresses many of the shortcomings of the classical distillation method described above. First, we incorporate a composition-explicit data channel for each distillate fraction (for qualitative, quantitative and trace analysis). Sampling very small distillate volumes (5–25 μL) yields a composition-explicit data channel with nearly instantaneous composition measurements. Chemical analysis of the distillate fractions allows for determination of how the composition of the fluid varies with volume fraction and distillation temperature, even for complex fluids. These data can be used to approximate the vapor liquid equilibrium of complex mixtures, and presents a more complete picture of the fluid under study. The ADC approach provides consistency with a century of historical data, an assessment of the energy content of each distillate fraction, and, where needed, a corrosivity assessment of each distillate fraction. Suitable analytical techniques include gas chromatography with either flame ionization detection (GC-FID) or mass spectral detection (GC-MS), element-specific detection (such as gas chromatography with sulfur or nitrogen chemiluminescence detection, GC-SCD or GC-NCD), and Fourier transform infrared spectrometry (FTIR) [9, 10].

Another advantage of the ADC approach is that it provides temperature, volume and pressure measurements of low uncertainty, and the temperatures obtained are true thermodynamic state points that can be modeled with an equation of state. In fact, we have used the ADC method to develop chemically authentic surrogate mixture models for the thermophysical properties of a coal-derived liquid fuel, a synthetic aviation fuel, S-8, and the rocket propellants, RP-1 and RP-2 [11–13]. Such model development would not be possible with the ASTM D-86 approach because there is no link to theory. In other recent reviews, we have discussed the analytical and separation science aspects of the ADC method [14, 15]. In this review, we concentrate on the applications in fluid design and engineering.

## 2 ADC Method

The apparatus and procedure for the measurement of the composition ADC have been discussed in detail elsewhere; only a brief description will be provided here [7, 8]. The apparatus is depicted schematically in Fig. 1. The stirred distillation flask is placed in an aluminum heating jacket contoured to fit the flask. The jacket is resistively heated and controlled by a model predictive proportional-integral-derivative (PID) controller that applies a precise thermal profile to the fluid [16]. Three observation ports are provided in the insulation to allow penetration with a flexible, illuminated borescope. The ports are placed to observe the fluid in the boiling flask, the top of the boiling flask, and the distillation head (at the bottom of the take-off).

Above the distillation flask, a centering adapter provides access for two thermally tempered, calibrated thermocouples that enter the distillation head. One thermocouple (T1) is submerged in the fluid and the other (T2) is centered at the low point of distillate take-off. Also in the head is an inert gas blanket for use with thermally unstable fluids. Distillate is taken off the flask with a distillation head, into a forced-air condenser chilled with a vortex tube [17, 18]. Following the condenser, the distillate enters a new transfer adapter that allows instantaneous sampling of distillate for analysis. When the sample leaves the adapter, it flows into the calibrated, level-stabilized receiver for a precise volume measurement. Since the measurements of the distillation curves are performed at ambient atmospheric pressure (measured with an electronic barometer), temperature readings were corrected for what should be obtained at standard atmospheric pressure (1 atm = 101.325 kPa). This adjustment is done with the modified Sydney Young equation [19–22]. The typical temperature uncertainty is less than 0.3 °C, the volume uncertainty is 0.05 mL, and the uncertainty in the pressure measurement is 0.003 kPa.

To measure a distillation curve, fluid (40–200 mL) is placed in the distillation flask and the heating profile begins. The profile typically has the sigmoidal shape of a distillation curve, but continuously leads the fluid by ~20 °C. For each ADC measurement, we can record a data grid consisting of: $T_k$, the temperature of the fluid (measured with T1), $T_h$, the temperature in the head (measured with T2), the corresponding fluid volume, the elapsed time, and the external (atmospheric) pressure. Along with these data, one withdraws a sample for detailed analysis. This procedure provides access to the detailed composition, energy content [23], corrosivity [24–27], etc., corresponding to each datum in the grid.

  

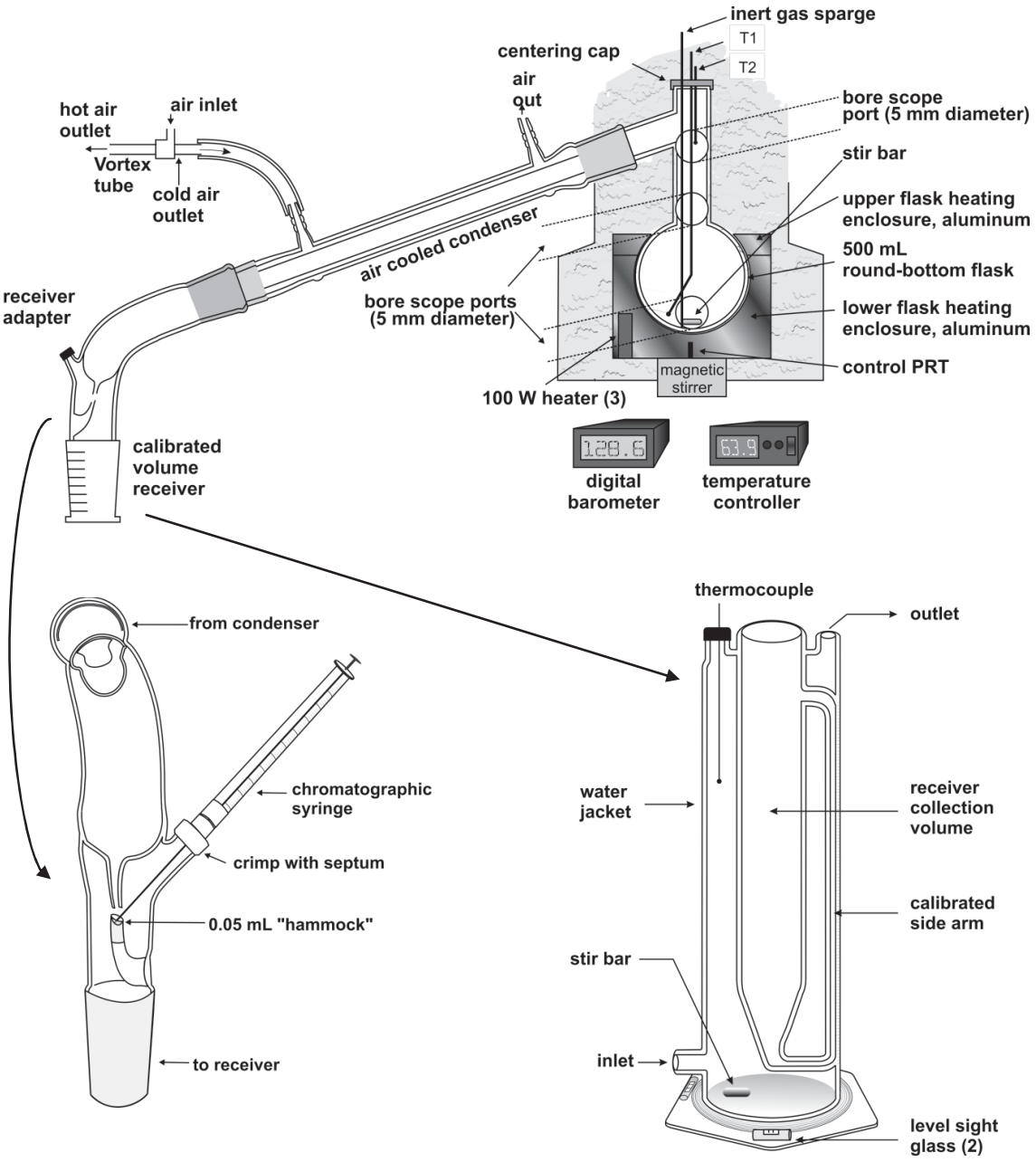


**Figure 1.** Schematic diagram of the overall apparatus used for the measurement of distillation curves. Expanded views of the sampling adapter and the stabilized receiver are shown in the lower half of the figure.

## 3 Examples of Measurements and Applications

### 3.1 Volatility and Composition

In this section, we illustrate the applications of the ADC with selected examples that relate the volatility (measured by the temperature data grid) to the distillate fraction composition, all for the specific purpose of fluid design. We will begin with work done on fuels for rocket motors and then move to automotive and jet engine fuels.

While modern rocket motors can operate on either a liquid or a solid fuel package, the former is more easily controlled and flexible. This led to the development of RP-1 kerosene in the 1950s, which continues to be widely used [28]. The desire in recent years to use rocket motors many times has led to reformulations of RP-1 with low sulfur, olefin and aromatic content. Reformulation has required a reassessment of the physical properties, for which we have used the ADC metrology. We show in Fig. 2 a distillation curve of RP-1 that has the composition measurement superimposed [29, 30]. First, focusing on the plot of $T_k$ against the volume fraction, we note that the

  

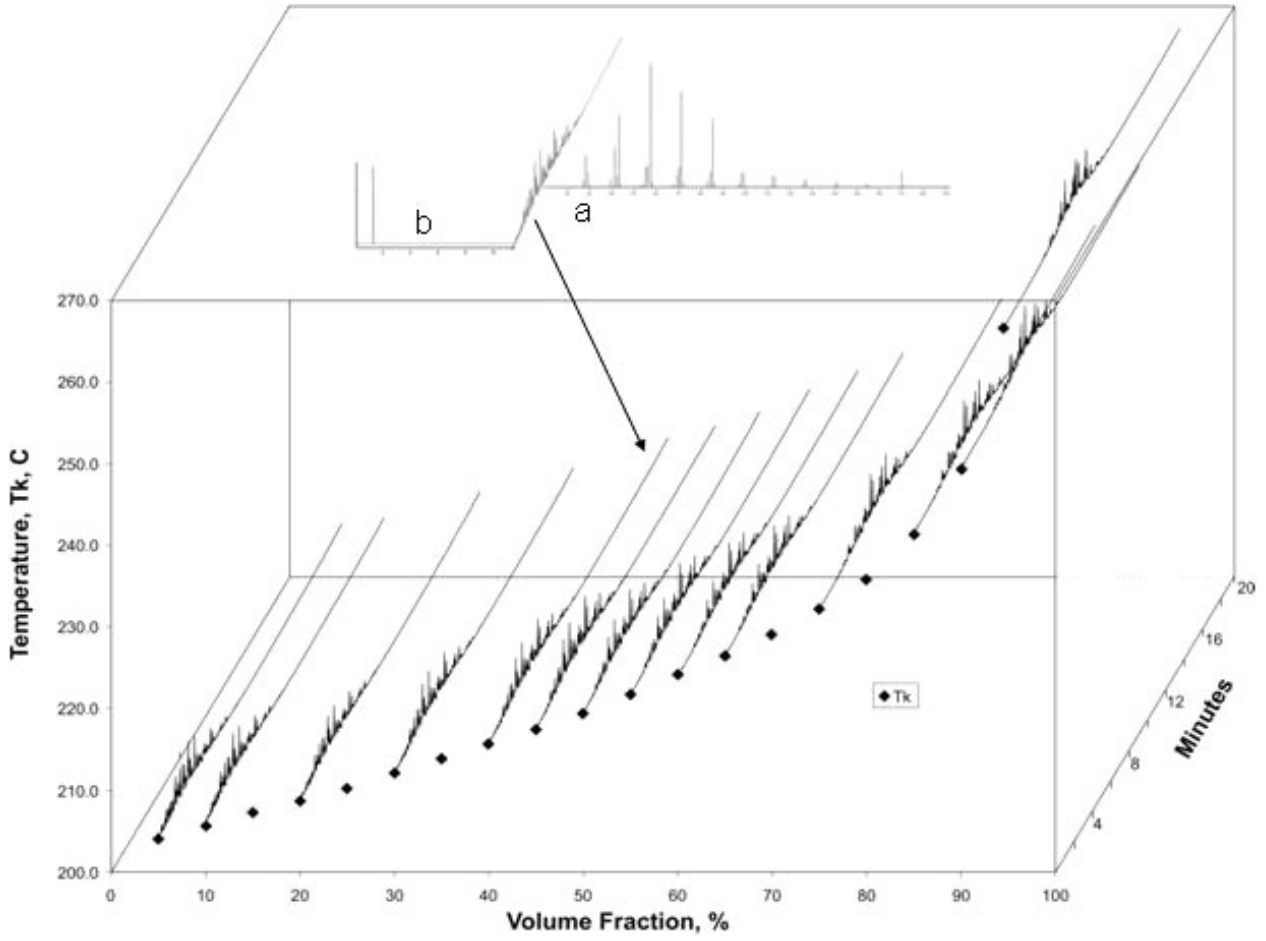


**Figure 2.** Distillation curve for RP-1 showing $T_k$ against the volume fraction in the *x*-*y* plane, and the composition as measured by gas chromatography along the "*z*"-axis, represented as retention time against peak intensity. Inset (a) above shows the mass spectrum of the major peak of the 40 % fraction, *n*-dodecane; inset (b) shows a total sulfur chromatographic peak.

plot shape is a subtle sigmoid, characteristic of a complex fluid with many components. ADC data such as these are used in the design and specification of many engine operational parameters, and in equation of state development. Since the $T_k$ data are thermodynamic state points, the plot represents a cut through the fluid phase diagram that has theoretical meaning.

The composition-explicit channel provides additional information for the data grid. In Fig. 2, the composition is shown for selected temperature-volume pairs by GC-MS. Additional detail is shown in the inset, where the mass spectrum of the largest peak is identified as *n*-dodecane, and a sulfur analysis done with a split to a GC-SCD. What is most significant is that this compositional information is now joined with a temperature grid measurement as discussed above; the temperature, pressure and composition can all be modeled with an equation of state, as discussed later.

We can further illustrate the value of relating the composition of distillate to the distillation curve temperatures by considering measurements performed on a series of samples taken from a fuel ethanol plant. In the USA, most fuel ethanol is made from corn, 75 % of which is processed by dry milling [31]. Outside the USA, the largest producer and user of fuel ethanol is Brazil, where the primary feedstock is cane sugar [32]. We applied the ADC to the product fluids from sample points of a modern Brazilian ethanol plant [33]. The overall flow diagram for this plant is provided in Fig. 3. The locations at which samples were drawn for this work are shown in the inset circles, labeled 1 through 5. In this plant, the first and second distillation columns (noted as stripping and rectification) operate at a slight pressure difference. The second distillation column produces the azeotropic concentration of ethanol in water, typically 94 wt % ethanol. In the past, further dehydration to fuel ethanol was done with the addition of benzene or cyclohexane to break the azeotrope, and subsequent distillation [34–36]. Modern plants use molecular sieve dehydration, resulting in lower energy consumption. Although only one molecular sieve unit is shown in Fig. 3, multiple units operate so that regeneration can be done without taking the entire plant off-line.

The feedstock from the fermenter is called the wine, shown as sample point 1. This fluid typically consists of an aqueous solution of 6.5 wt % ethanol, and is a dark reddish brown in

  

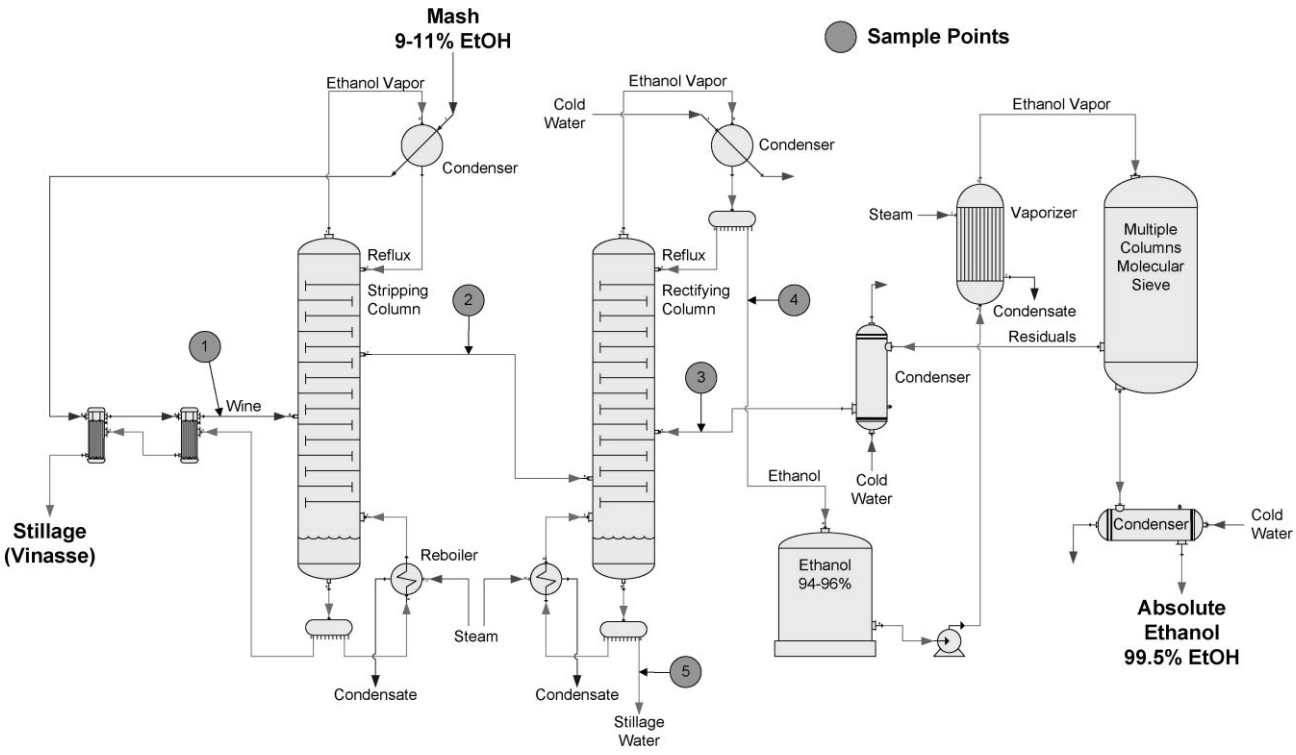


**Figure 3.** Flow diagram showing the essential features of the ethanol plant from which the samples measured in this work were taken. The sample points at which fluid was withdrawn for the measurement of distillation curves are indicated, numbers 1–5.

color with a distinct odor of molasses. Unlike the other fluids in the process stream, this fluid typically has solids in suspension and will often show variability due to the weather conditions during the growing season. In Fig. 4, we present the distillation curve of a typical wine, and we note that the distillation temperatures are initially indicative of the presence of ethanol (approximately 94 °C); by the 20 % distillate fraction, this is now essentially water. Also presented is the measured ethanol concentration from the composition-explicit channel of the ADC. This was measured by GC-FID. Also mea-

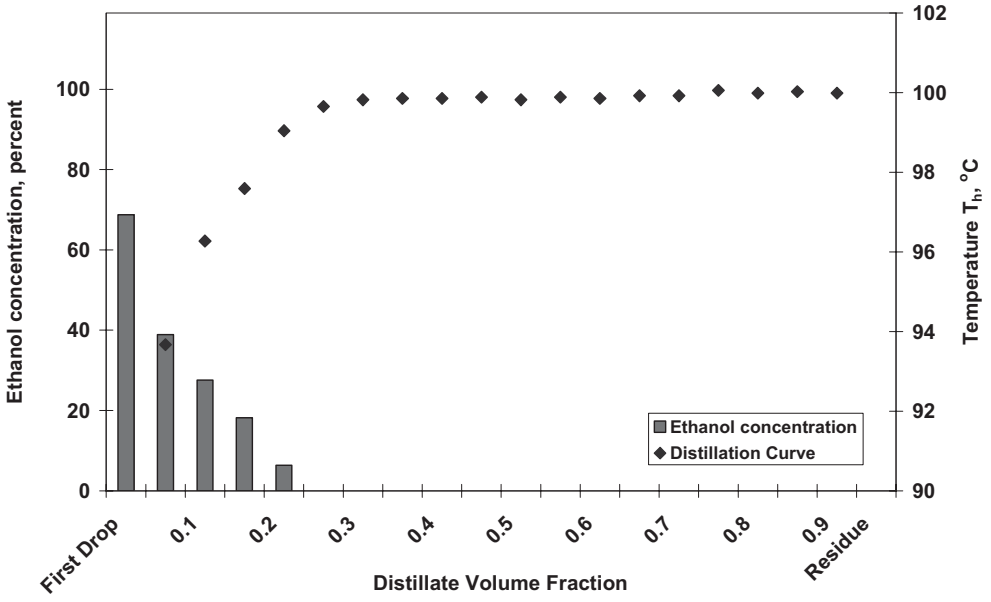


**Figure 4.** Representative distillation curve, presented as $T_h$, of the wine sample taken at position 1 in Fig. 3. Also presented is the measured ethanol concentration (wt %).

  

sured, but not shown here, was the water content as a function of distillate cut, measured with Karl Fisher coulombic titrimetry. We note that the first drop of distillate has an ethanol concentration of nearly 70 wt %, and this concentration drops as the distillation proceeds, corresponding to the distillation curve. The temperature and composition information for each of the sampling points are needed for an effective modeling of the plant.

### 3.2 Volatility and Energy Content

The ability to apply a detailed quantitative analysis to each distillate fraction offers the potential of assessing thermal properties such as the energy content of a fuel. If the enthalpy of combustion is known (or predictable) for the components of a mixture, the composite enthalpy of combustion of a mixture of these components can be derived (neglecting the enthalpy of mixing). We have demonstrated how this can be applied to the distillate fractions corresponding to the data grid of the distillation curve [23]. It is not necessary to identify all the components of the fraction; a substantial subset of the major constituents is adequate, and the uncertainty caused by the use of a subset is negligible [37–39].

In the comparison of aviation fuel properties, a major interest is clearly the energy content. We illustrate this with a comparison of different samples of Jet-A, which is the most common turbine aviation fuel used commercially in the USA, with a consumption of 800 billion L in 2006. The ADC was applied to three different batches of Jet-A (designated numerically as 3638, 3602 and 4658) that are thought to represent the composition gamut very well [39, 40]. The sample labeled 4658 is a composite of numerous batches (from multiple manufacturers and locations) of Jet-A mixed in approximately equal volume aliquots. It is therefore considered to be the most representative of the three samples. The sample labeled 3638 was known to be unusual in that the aromatic content was lower than that of typical batches, while that labeled 3602 was unremarkable and typical. We noted a divergence in the distillation curves of these three fluids at the 70 % fraction, so a quantitative analysis was done at this fraction for each fluid. We then applied our method to determine the enthalpy of combustion of this fraction, the results of which are shown as a histogram in Fig. 5, along with a comparison to the synthetic aviation fuel made from natural gas, S-8. We were surprised to note a significant spread in the enthalpy values among these fluids. The mixed sample shows the highest energy content, while the atypical fluid 3638 shows the lowest. The combination of the distillation data grid with the composition analysis and the enthalpic analysis permits a more complete understanding of the fuel properties and how they relate to composition.

### 3.3 Tracking Selected Components

Finished fuels often incorporate additives for specific purposes, including oxygenating agents, antiknock agents, extenders, preservatives, antifoam and lubricity agents, and detergents. While some of these are present at trace levels, others (especially oxygenates and extenders) are added in concentra-

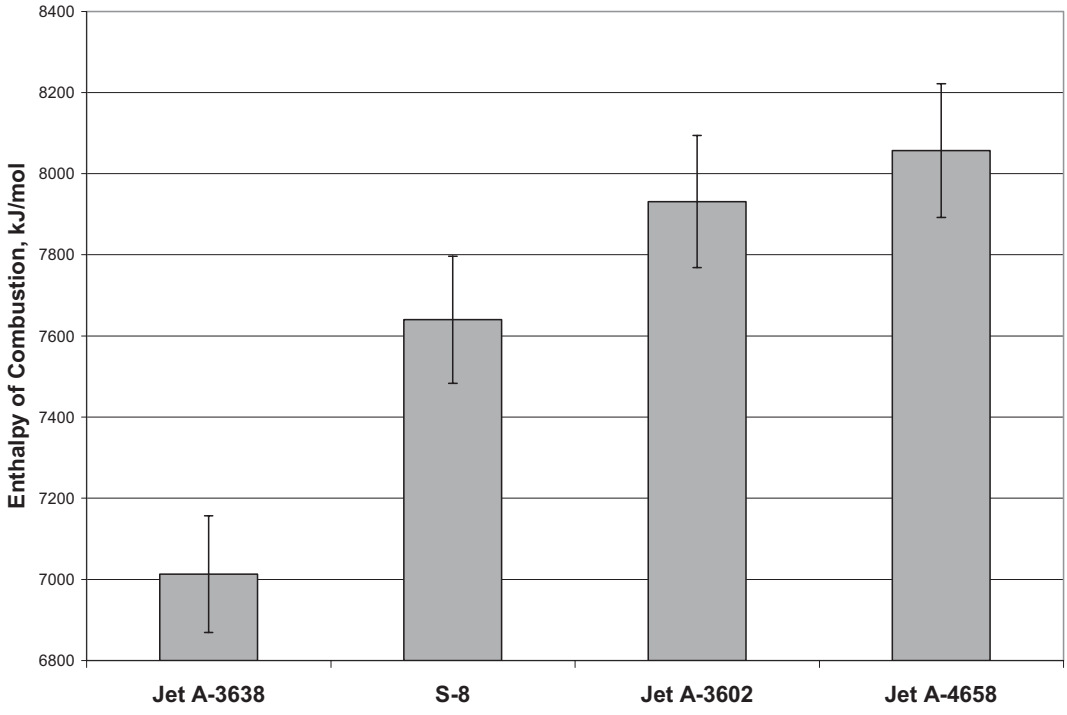


**Figure 5.** The composite enthalpy of combustion of the 70 % distillate fraction for three samples of Jet-A and the sample of S-8. The fluids are presented in increasing enthalpy of combustion of the 70 % distillate fraction.

  

tions of 10 % or higher. The development of models for the thermophysical properties of such fluids requires explicit knowledge of how the additives change the fundamental properties such as the volatility. We can use the ADC to unify these two important parameters: composition and thermophysical properties.

Oxygenates added to gasoline to reduce carbon monoxide emissions are familiar, but various oxygenates have been added to diesel fuel to decrease (or eliminate) particulate formation. We have measured numerous gasoline [41] and diesel fuel mixtures with oxygenates, including synthetics and biomass-derived fluids [42, 43]. Since many engine operation and environmental parameters depend on the distillation curve, the ability to relate the changing composition and actually model the fluid behavior is critical. In Fig. 6, we present the ADC results for mixtures of diesel fuel with three different concentrations of diethyl carbonate (DEC), a promising oxygenate [44]. DEC is used extensively as an ethylating agent in organic synthesis (for example, it is used in the synthesis of the anticonvulsant drug phenobarbital), and it is also used extensively as a solvent in the textile industry. It is biodegradable and insoluble in water. We note that, in mixtures with diesel fuel, DEC causes a significant inflection to lower temperatures. It is more volatile than most of the diesel fuel components, and even at a starting concentration of 30 vol.-%, it has been removed from the diesel fuel by the 0.5 distillate fraction, at which point the distillation curve of the DEC mixture is approaching (but not merging with) that of diesel fuel. This is reflected in the inset, in which a quantitative analysis of the DEC in the distillate is provided, having been measured by GC-FID. Especially interesting is that the additive, although removed by a distillate fraction of 0.5, still apparently has an effect on the vapor liquid equilibrium (VLE) late in the distillation. The vaporization of the lighter components of diesel fuel, which would ordinarily be found early in the distillation curve, is delayed by the presence of the additive. We will discuss this in more detail later in the section on thermodynamic modeling; however, it is precisely this combination of temperature and composition information that permits a more complete understanding of the behavior of such complex mixtures.

Another instructive example of how we can track an additive through the distillation curve (but this time an additive concentration approaching the trace concentration level) comes from the measurement of the commercial aviation gasoline, avgas 100LL. Although motor fuels used today do not contain lead additives, much general aviation gasoline (avgas 100LL) still contains tetraethyl lead (TEL, CAS No. 78-00-2). Since TEL was banned from motor gasoline, avgas is now one of the largest contributors of lead in the atmosphere in many locations. Significant efforts have been made to develop a low-cost, lead-free alternative fuel to replace avgas 100LL for aircraft that use piston engines. The examination of avgas 100LL with the ADC provides the opportunity to ultimately develop an equation of state for avgas and to track the presence of the lead

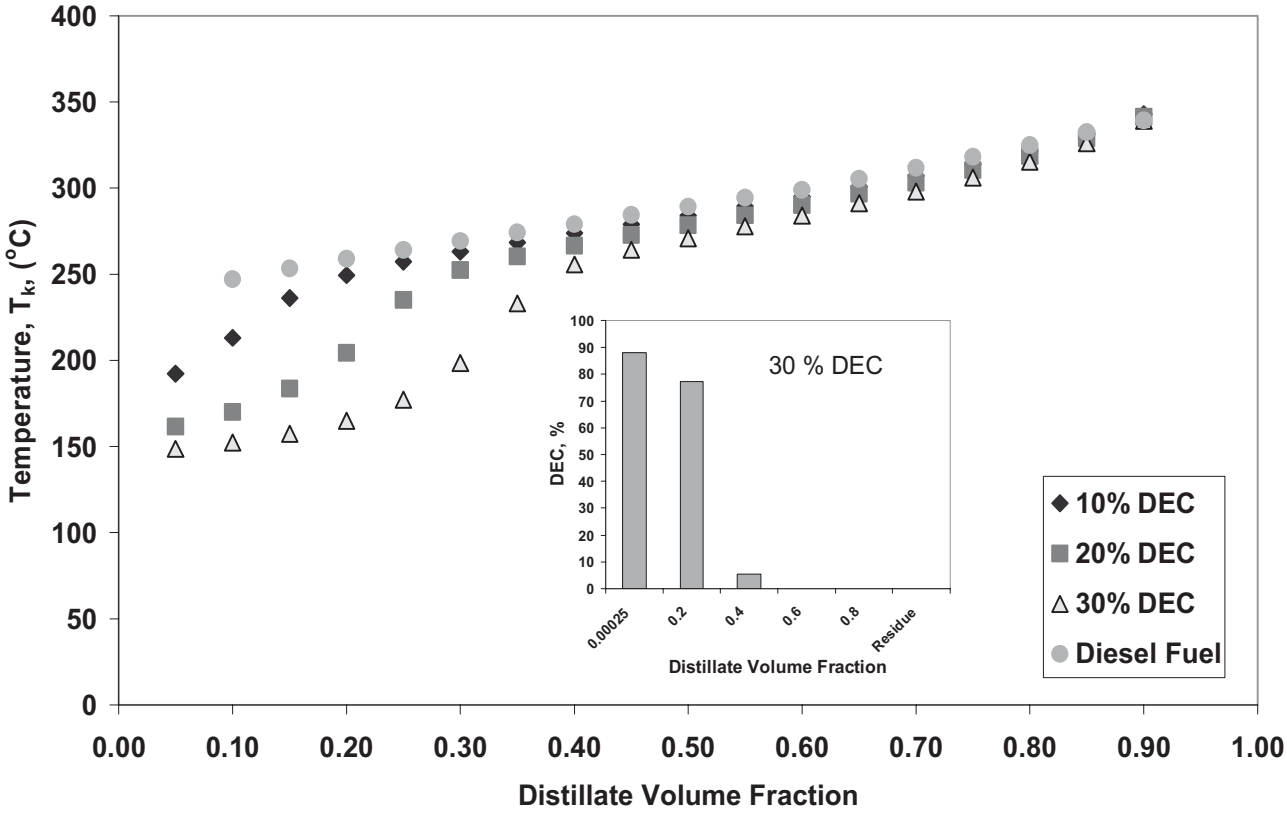


**Figure 6.** Distillation curves of diesel fuel and diesel fuel with 10, 20, and 30 vol.-% of DEC. The inset shows the concentration profile (in wt %) of the additive as a function of the distillate cut.

  

compound through the full range of the distillation curve. In Fig. 7, we apply the ADC to avgas 100LL [45]. The *y*-axis presents the thermodynamically consistent temperatures. In inset (a) we present the enthalpy of combustion as a function of the distillate cut (from a quantitative analysis of each fraction). This allows the energy content to be related to the other fuel properties. In inset (b), we present the composition profile of TEL as a function of the distillate cut, which comes from specific trace analysis applied to the distillate cuts. We note that there is far more TEL in later distillate fractions.

### 3.4 Detection and Study of Azeotropes

Azeotropic mixtures are among the most fascinating and at the same time the most complicated manifestations of phase equilibrium. They also play a critical role in many industrial processes (and the resulting products), especially separations.

As we noted earlier, the ADC measures two temperatures, $T_k$ and $T_h$. Typically, during the measurement of a complex, multicomponent fluid, the $T_k$ measurement is higher than the $T_h$ measurement by several (5–15) degrees. This must be the case since the mass transfer-driving force comes from the temperature differential between the kettle and the head. If one performs an ADC measurement on a pure fluid, the temperature difference between $T_k$ and $T_h$ is very small, no more than 0.1 °C; the composition does not change during the distillation. Moreover, the curve for a pure fluid is flat with no slope. We would expect this difference in temperature differential and slope to be reflected in the distillation of an azeotrope, because where azeotropic pairs are present, the mixture behaves as a pure fluid. Mixtures of gasoline oxygenates in fact show this behavior since the lower alcohols form azeotropes with many of the hydrocarbon components in gasoline [38]. In Fig. 8a, we show the distillation curves of a 91 AI (antiknock index) premium, winter-grade gasoline, presented in $T_k$ and $T_h$. This fuel has no added oxygenate. We note for this complex, multicomponent fluid that $T_k$ is always higher than $T_h$ by an average of 6.2 °C. In Fig. 8b, we show the same gasoline with 15 vol.-% methanol. Two features are noteworthy. First, we observe a flattening of the curve for distillate volume fractions up to approximately 40 %, relative to that for the straight gasoline. This persists until the methanol has been distilled out of the mixture. Second, we also note the convergence of $T_k$ and $T_h$ in this region, which we have called the azeotropic convergence. Here, the difference between $T_k$ and $T_h$ averages 0.3 °C, while subsequent to the azeotropic inflection, the difference increases to an average of 8.6 °C.

We can take the examination of azeotropes to a more fundamental level by examining some well-known binary mixtures. One of the best-studied mixtures is the minimum boiling binary azeotrope that is formed by benzene and ethanol. It is often presented in introductory texts as an instructional example because of the striking features and structure of the phase dia-

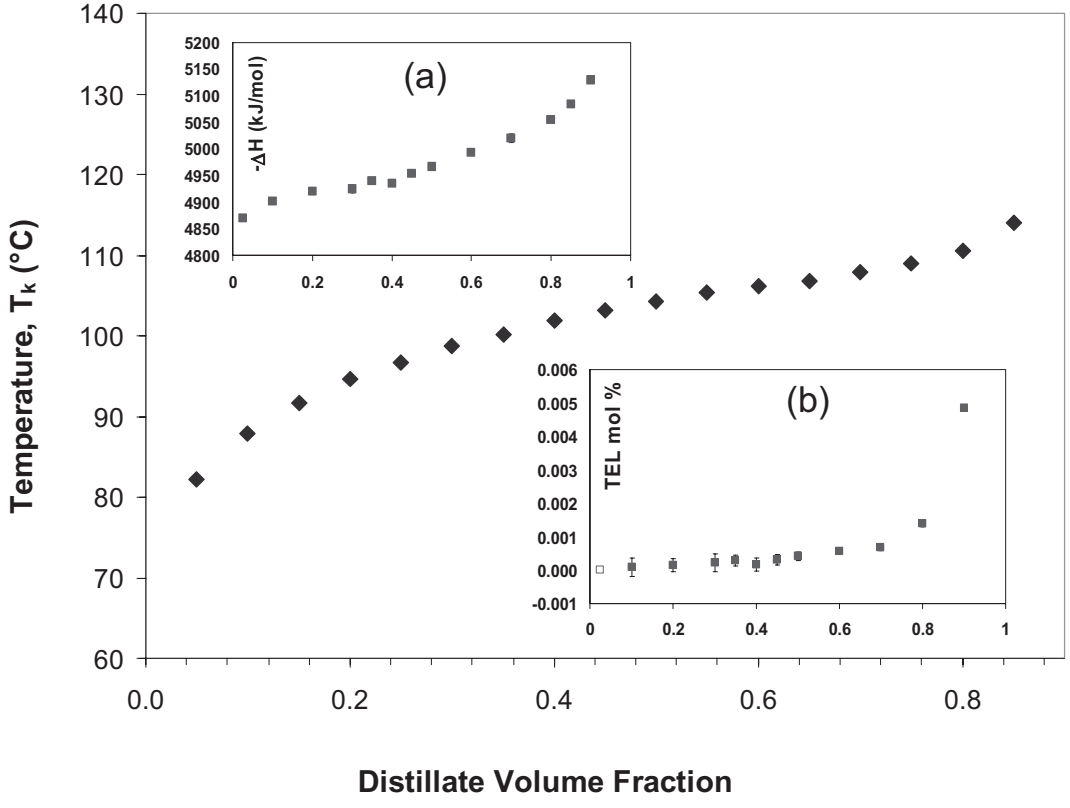


**Figure 7.** Distillation curve of avgas 100LL with the enthalpy of combustion in inset (a) and the concentration of TEL in inset (b), both as a function of the distillate cut.

  

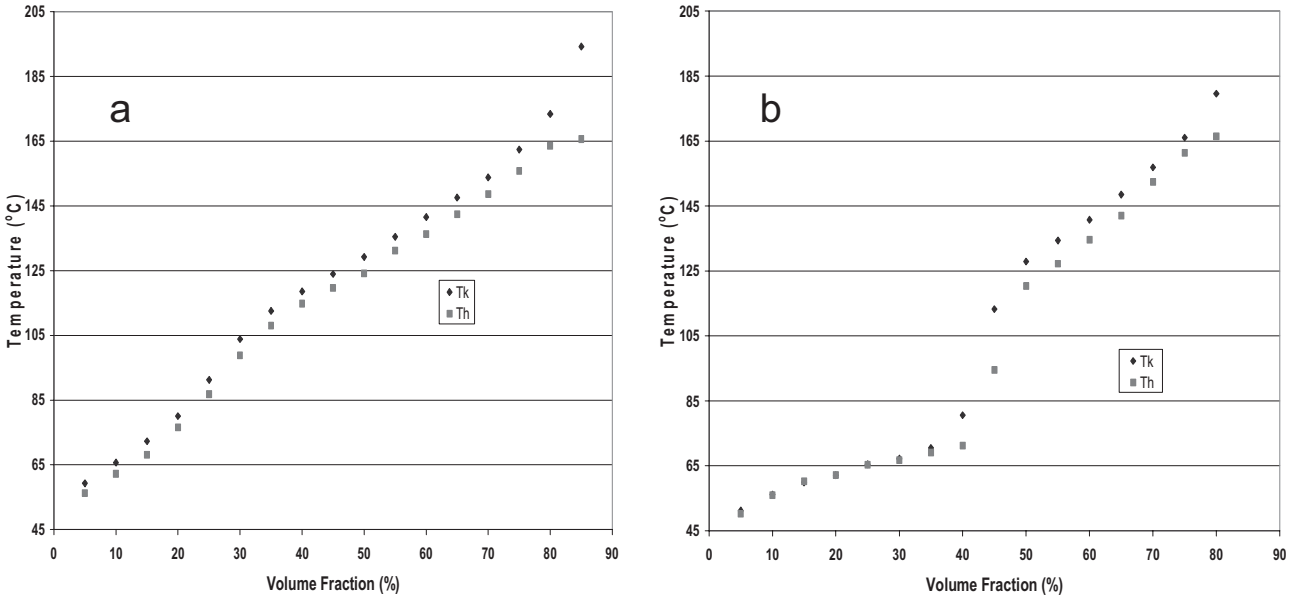


**Figure 8.** Distillation curves of (a) 91 AI gasoline and (b) 91 AI gasoline with 15 vol.-% of methanol. The azeotropic convergence is caused by pairs of azeotropes forming between methanol and some components of gasoline.

gram (the temperature differences are significant, the two-phase region is large, and the azeotrope occurs nearly at the midpoint of the *T-x* diagram). This mixture is also industrially important in the formulation and design of oxygenated and reformulated gasolines. The *T-x* phase diagram of this binary, shown in the inset of Fig. 9, is anchored on the left side by the pure ethanol point (at a normal boiling temperature of 78.4 °C) and on the right side by the pure benzene point (at a normal boiling temperature of 80.1 °C) [46]. The bubble and dew point curves meet at the minimum located at 68.2 °C. Centered about the minimum on the bubble point curve is a relatively flat region where the slopes in either direction are gentle. These slopes become increasingly more pronounced as one proceeds away from the azeotrope. The dew point curves proceed from the azeotropic point to the pure component points in a more linear fashion with relatively constant slope.

Distillation curves are presented in Fig. 9 for binary mixtures with starting compositions of 0.20, 0.40, 0.55, 0.70 and 0.80 mole fraction of benzene ($x_b$) [46]. We note that the distillation curves for the starting compositions $x_b$ = 0.20 and 0.40 converge at a temperature of 78.9 °C, while those at $x_b$ = 0.70 and 0.80 converge at a temperature of 80.9 °C. These two different families of curves, which begin with starting compositions on either side of the azeotrope, converge to the appropriate pure component: 78.9 °C (for $x_b$ = 0.20 and 0.40, converging to ethanol) and 80.9 (for $x_b$ = 0.70 and 0.80 converging to benzene). We note that the shapes of the curves for $x_b$ = 0.20 and 0.80 are initially far steeper than those for $x_b$ = 0.40 and 0.70. This can be explained with reference to the *T-x* diagram. We note that the initial steepness of slope corresponds with the pronounced increase in slope of the bubble point curve. Where the *T-x* diagram is steep, the distillation curve is correspondingly steep. This shape gives an indication of the deviations from Raoult's law, with steeper curves indicating larger deviations. For the mixture starting at a benzene mole fraction of 0.55, we note that the distillation curve is flat, behaving as a pure fluid at the azeotrope. We also note that the liquid and vapor compositions are the same. The ADC thus provides a simple and rapid avenue to the study of azeotropic mixtures. Each such curve can be completed in 1 h with relatively simple instrumentation, whereas the *T-x* diagram would require many hours to measure in a specialized VLE apparatus.

### 3.5 Volatility and Chemical Stability

Biodiesel fuel has been the focus of a great deal of media attention and scientific research in the last several years as a potential replacement or extender for petroleum-derived diesel fuel. The major constituents (fatty acid methyl esters, FAME) of pure biodiesel are generally relatively few, consisting mainly of methyl palmitate, methyl stearate, methyl oleate, methyl linoleate, and methyl linolenate. As a fuel for compression ignition engines, biodiesel fuel has several advantages (renewable, high increased lubricity, non-carcinogenic, non-mutagenic, biodegradable, decreased carbon monoxide, unburned hydrocarbon, and particulate-matter emission). There are also some serious disadvantages to biodiesel fuel (increased $NO_x$ emissions, moisture absorption during storage, and chemical instability). The last item is especially problematic at higher temperatures, although the instability in storage has received more attention. We found in earlier work on biodiesel fuel (B100) that the thermal and oxidative instability of this fluid prevented the measurement of a distillation curve with our usual ADC approach; discrepancies in temperature of up to 20 °C were ob-

  

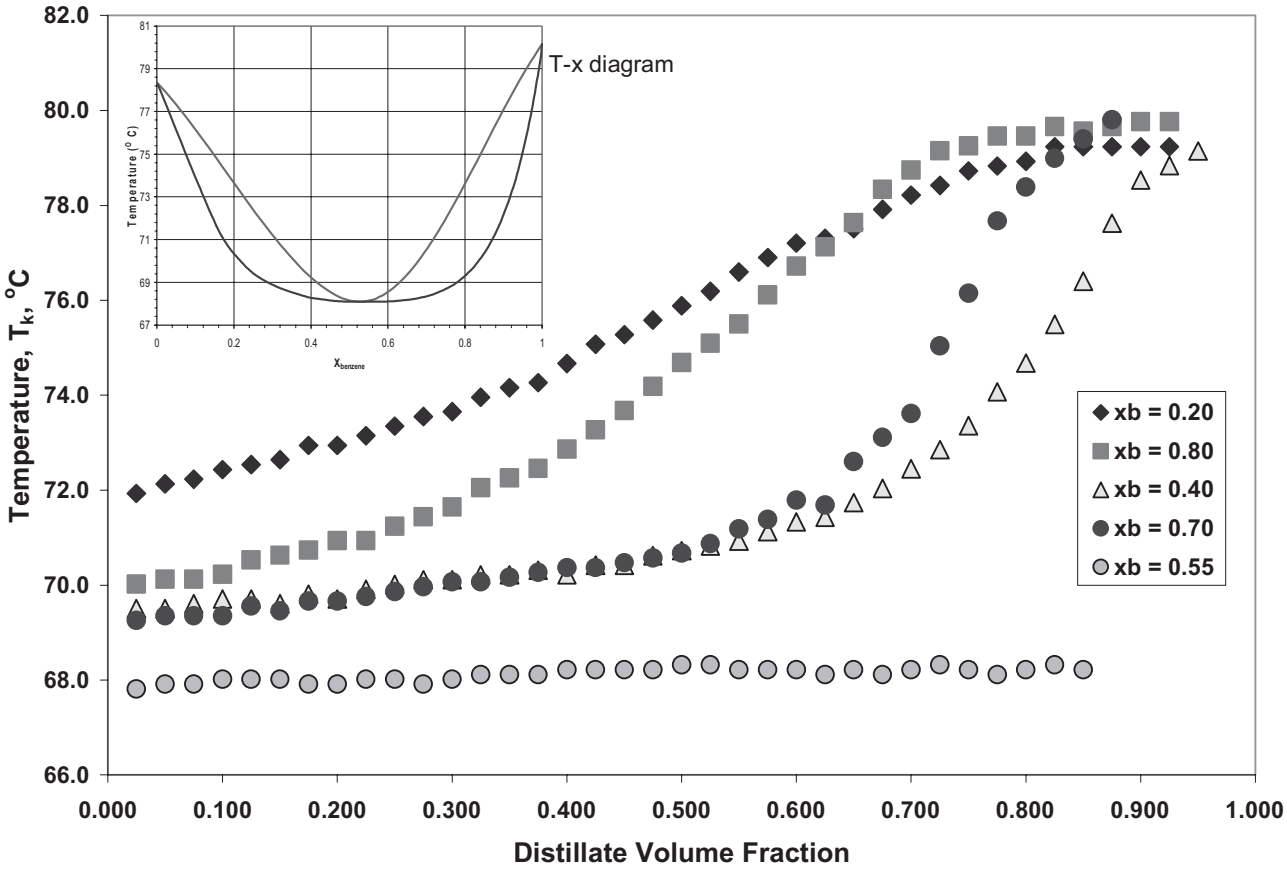


**Figure 9.** Plot of the distillation curve data for binary mixtures of ethanol + benzene at benzene mole fractions $x_b$ = 0.20, 0.40, 0.55, 0.70 and 0.80. The inset shows the familiar *T-x* diagram for this mixture. The azeotrope exists at a benzene mole fraction of 0.55.

served between successive measurements. The addition of an argon gas sparge incorporated into the distillation flask eliminated the problem and allowed the measurement of highly reproducible distillation curves. Since it is possible to quantitatively assess the "tightening" of replicate distillation curve measurements upon the addition of the sparge, we can use this change as a means of assessing the thermal and oxidative stability of the fluids being measured. We used three statistical descriptors of the improved curve-to-curve repeatability: the average range in temperature, the average standard deviation in temperature, and the area subtended for replicate measurements. We found that these measures correlated quantitatively with improved thermal and oxidative stability and thus provide a measure of stability.

We then used the ADC as described above to test the efficacy of stabilizing additives on sensitive fluids such as B100 [47, 48]. In particular, we tested three hydrogen donor additives: tetrahydroquinoline (THQ), *t*-decalin and tetralin (the classical donor solvent is composed of a saturated ring attached to an aromatic ring). Hydrogen donors are fluids or solvents that are capable of providing hydrogen to enable the conversion of heavier residuals into distillable fractions. They act to capture or sequester aliphatic radicals formed at temperatures in excess of 300 °C, and typically form C2 and C3 alkyl aromatic compounds. In Fig. 10, we present the distillation curve of B100 stabilized with 1 vol.-% THQ, and note that the repeatability of three successive curves is approximately 1.6 °C. This is a significant improvement from the unstabilized fluid (although not as significant as with the argon sparge). We track the concentration of THQ in the distillate in the inset, with the composition-explicit data channel of the ADC. We note that the stabilization effect is greatest earliest in the curve when the concentration of THQ is highest. The THQ decomposes and also distills out of the mixture during the course of the distillation, and its effect naturally decreases. Of the three stabilizers examined, THQ and *t*-decalin perform similarly; tetralin also resulted in stabilization, but with less effectiveness. Interestingly, this result parallels kinetics measurements performed on aviation fuels stabilized with these additives [49, 50].

### 3.6 Thermodynamic Modeling

Thus far in the discussion, we have focused on the analytical applications of the ADC. An important contribution to the concept of petroleomics, however, is the ability to use the information to advance the applied theory of complex fluids so as to describe and predict the physical properties of the mix-

  

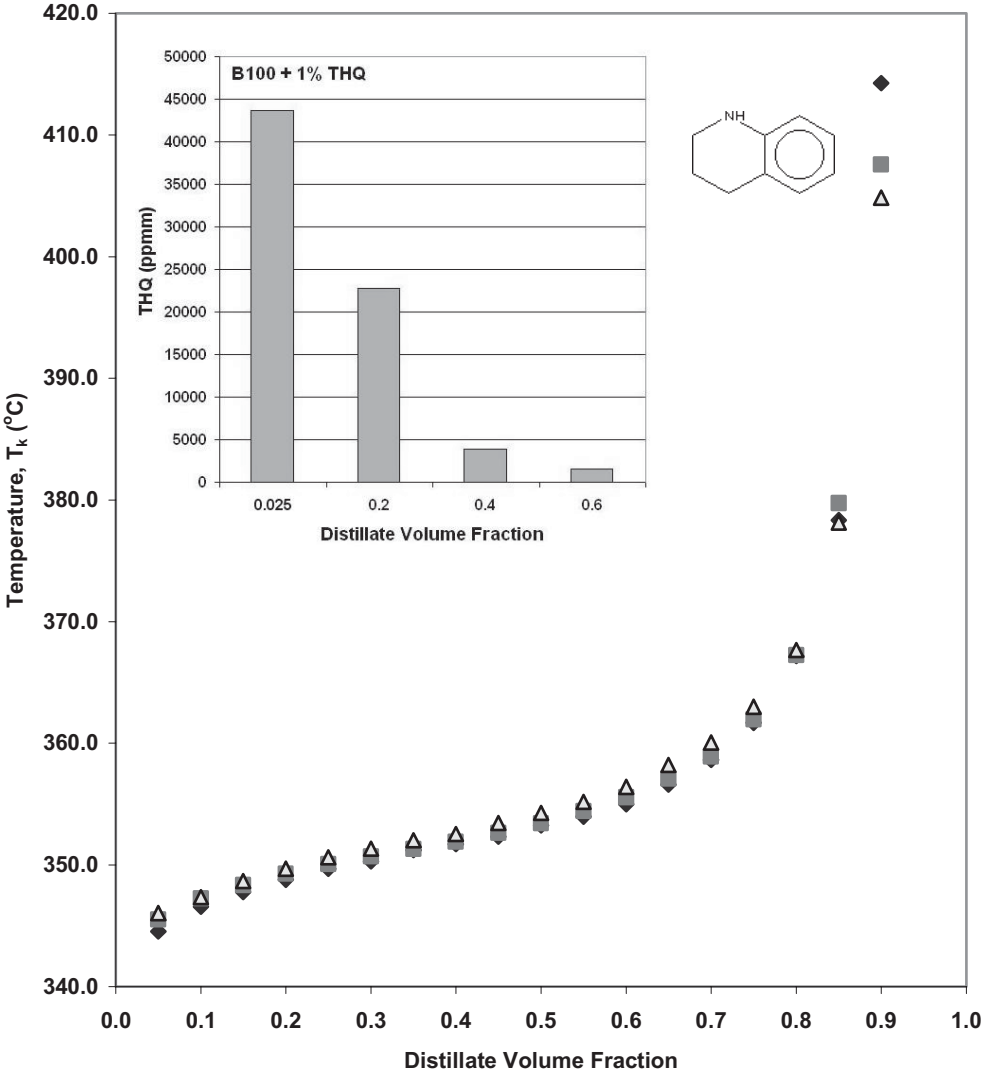


**Figure 10.** Three successive distillation curves of B100 biodiesel fuel with 1 % THQ (structure provided) stabilizing additive. The inset tracks the concentration (in ppm by mass) of THQ present in the distillate.

ture and its components. This has been largely missing from petroleomics. Since the ADC produces thermodynamically consistent temperatures along with the relevant composition picture, it is ideally suited for the development of such complex fluid theory. The basic idea in our approach is to represent the molar Helmholtz energy, $a$, of a mixture as a sum of an ideal contribution, $a^{\mathrm{idsol}}$, and an excess contribution, $a^{\mathrm{excess}}$:

$$a = a^{\mathrm{idsol}} + a^{\mathrm{excess}} \tag{1}$$

$$a^{\mathrm{idsol}} = \sum_{j=1}^{m} x_{\mathrm{i}} \left[ a_{\mathrm{i}}^{0}(\rho, T) + a_{\mathrm{i}}^{\mathrm{r}}(\delta, \tau) + RT \ln x_{\mathrm{i}} \right], \tag{2}$$

$$a^{\mathrm{excess}} = RT \sum_{i=1}^{m-1} \sum_{j=i+1}^{m} x_{\mathrm{i}} x_{\mathrm{j}} F_{\mathrm{ij}} \sum_{k} N_k \delta^{\mathrm{d_k}} \tau^{\mathrm{t_k}} \exp(-\delta^{\mathrm{l_k}}) \tag{3}$$

where $\rho$ and $T$ are the mixture molar density and temperature, $\delta$ and $\tau$ are the reduced mixture density and temperature, $m$ is the number of components, $a_{\mathrm{i}}^{0}$ is the ideal gas Helmholtz energy of component $i$, $a_{\mathrm{i}}^{r}$ is the residual Helmholtz energy of component $i$, $x_{\mathrm{i}}$ are the mole fractions of the constituents of the mixture, $d_{\mathrm{k}}$, $t_{\mathrm{k}}$, $l_{\mathrm{k}}$ and $N_{\mathrm{k}}$ are coefficients found from fitting experimental data, $F_{\mathrm{ij}}$ is an interaction parameter, and $R$ is the universal gas constant. Mixing rules are used to determine the reducing parameters $\rho_{\mathrm{red}}$ and $T_{\mathrm{red}}$ for the mixture, which are defined as:

$$\delta = \rho / \rho_{\mathrm{red}} \tag{4}$$

$$\tau = T_{\mathrm{red}} / T \tag{5}$$

$$\rho_{\mathrm{red}} = \left[ \sum_{i=1}^{m} \frac{x_{\mathrm{i}}}{\rho_{c_{\mathrm{i}}}} + \sum_{i=1}^{m-1} \sum_{j=i+1}^{m} x_{\mathrm{i}} x_{\mathrm{j}} \xi_{\mathrm{ij}} \right]^{-1} \tag{6}$$

  

$$T_{red} = \sum_{i=1}^{m} x_i T_{c_i} + \sum_{i=1}^{m-1} \sum_{j=i+1}^{m} x_i x_j \varsigma_{ij} \quad (7)$$

where $\xi_{ij}$ and $\zeta_{ij}$ are binary interaction parameters that define the shapes of the reducing temperature and density curves, and $T_{red}$ and $\rho_{red}$ are the reduced temperature and density.

The model has three binary interaction parameters for each component pair, $\xi_{ij}$, $\zeta_{ij}$, and $F_{ij}$, which can be determined by fitting experimental data. Since the constituent fluids are chemically similar, we set the excess contribution to zero (i.e., $F_{ij} = 0$), and the $\xi_{ij}$ interaction parameter to zero, resulting in a simpler model with only one binary interaction parameter, $\zeta_{ij}$. Previous studies on refrigerant mixtures have shown that $\zeta_{ij}$ is the most important binary parameter. This parameter can be found by fitting binary mixture data, or when data are unavailable, the following predictive scheme is used:

$$\varsigma_{ij} = \frac{T_{c_2}}{T_{c_1}}(40.4 - 25.03 \cdot 2^s) \quad (8)$$

$$s = \left(\frac{T_{c_1}}{T_{c_2}} \frac{p_{c_2}}{p_{c_1}} \frac{\omega_2}{\omega_1}\right) \quad (9)$$

where the fluid with the smaller dipole moment is designated as fluid "1", and $\omega$ is the acentric factor.

The model for calculating the transport properties of a mixture is an extended corresponding-states method. In this approach, the viscosity or thermal conductivity of a mixture is calculated in a two-step procedure. First, mixing and combining rules are used to represent the mixture in terms of a hypothetical pure fluid, then the properties of the hypothetical pure fluid are determined by mapping onto a reference fluid through the use of "shape factors"; details are given elsewhere. For both refrigerant mixtures and mixtures of natural gas components, the viscosity and thermal conductivity are typically represented to within 5–10 %. The two models discussed briefly above, the Helmholtz-energy mixing model for thermodynamic properties and the extended corresponding-states model for viscosity and thermal conductivity, are implemented in NIST's REFPROP computer program [51]. This program contains highly accurate equations of state for pure fluids, including some adopted as international standards [52].

We can use the theoretical formalism presented above in different ways. First, we can correlate experimental property data, producing a model to represent the data within experimental uncertainty. Second, we can use the model predictively to estimate property values, based on limited experimental data. With the ADC as a primary experimental input, we have used both of these approaches.

Returning to the synthetic aviation fuel S-8 discussed earlier, we can represent the composition of the fluid with a surrogate mixture with components representing families of compounds found in S-8. Then, correlating measured density, heat capacity, sound speed, viscosity and thermal conductivity, it is possible to model the properties of the mixture. Without the ADC as an input, however, the ability of the model to represent volatility is severely flawed. We show in Fig. 11a the experimental measurements and calculated distillation curves obtained with the Helmholtz model with and without the ADC data as an input [11]. Including the distillation curve in the model development allows correlation of the volatility to within experimental uncertainty, while failing to do so results in a physically unrealistic representation.

We can also use the formalism presented above in a predictive fashion, whereby we use a chemical analysis along with the ADC to predict the remaining physical property information (density, sound speed and viscosity). As an example, we study another synthetic substitute for JP-8, a blended coal-derived fluid (CDF) made from a significant fraction of coal liquids and light cycle oil, a by-product of catalytic cracking units in petroleum refining [13, 53]. The resulting mixture was treated

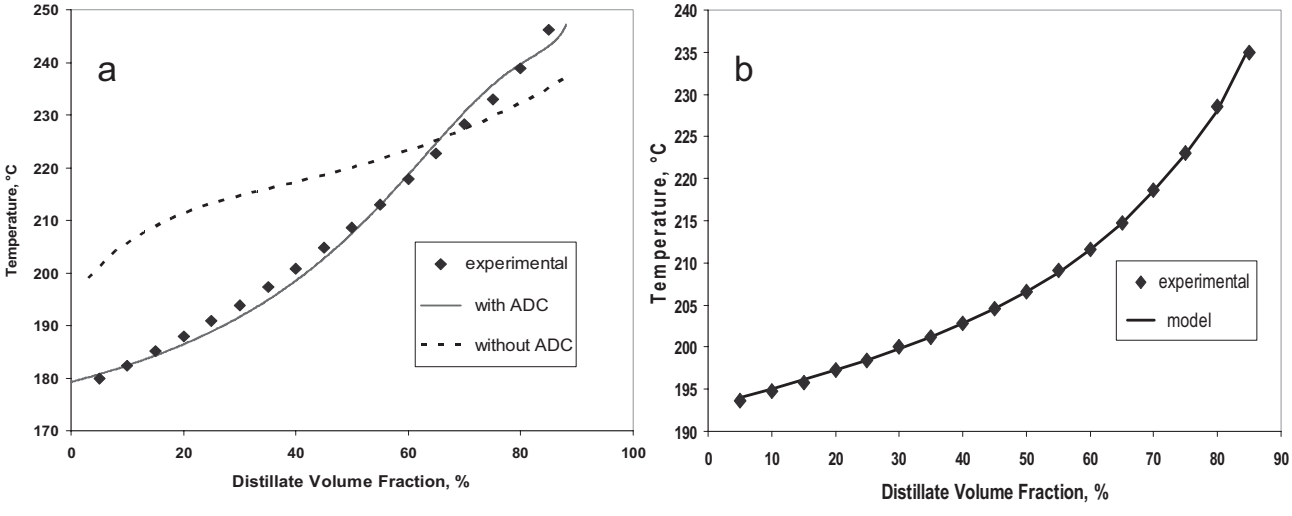


**Figure 11.** Plot showing the distillation curves modeled with the Helmholtz equation of state as compared with experimental data. The plot shown in (a) is for the synthetic aviation turbine fuel S-8, made from natural gas, and shows the model with and without the incorporation of the ADC data. The plot shown in (b) is for a coal-derived liquid turbine fuel in which the Helmholtz equation of state is used predictively to generate the distillation curve.

  

to increase the number of carbon-hydrogen bonds by hydroprocessing at high temperature and pressure. The fluid is intended for high chemical stability up to 480 °C (900 °F, hence the alternative name of the prototype, JP-900). The chemical analysis allowed the development of a five-component surrogate, and the resulting mixture model predicted the distillation curve very well, as shown in Fig. 11b. Moreover, the mixture model can represent other physical properties to within experimental uncertainty, realizing that such data are very limited.

In the discussion earlier on the oxygenating additives for diesel fuel, we noted that, in some cases, the additive has an effect on the volatility even after the additive has been completely removed (by distillation) from the mixture. This was illustrated with DEC, but we have observed the same effect with many more volatile additives that vaporize early in the distillation. This occurs because the energy being applied to the solution during the distillation is being used to vaporize the additive, and the lighter components of the fluid undergo delayed vaporization. We can use the thermodynamic models to demonstrate this and to predict the vaporization of the relevant species during the course of distillation. To do this we construct a very simplified surrogate mixture for diesel fuel and dimethyl carbonate (DMC), as listed in Tab. 1 [44]. We choose DMC for this illustration since the effect is dramatic and easily demonstrated on a plot. We can calculate the distillation curves for the three mixtures, and indeed the curves will not completely merge, even after the DMC has vaporized. Fig. 12a, b shows further calculations from our surrogate model, specifically tracking how the composition of the liquid and vapor phases change as the distillation proceeds. The compositions of DMC, *n*-nonane (the lightest component in the surrogate diesel) and *n*-hexadecane (the heaviest component in the surrogate diesel) are shown. Fig. 12a shows that the concentration of *n*-nonane is affected significantly by the additive, while *n*-hexadecane is affected to a much lesser extent. This behavior is shown for two initial concentrations of DMC (30 and 10 vol.-%), as described in Tab. 1. In Fig. 12, the peak in the vapor phase concentration of nonane is delayed so that the removal of *n*-nonane from the liquid phase is also delayed. The difference in the 10 and 30 % mixtures is dramatic, with the vaporization of *n*-nonane being delayed much later into the distillation than in the 30 % mixture. This results in the distillation curves approaching, but never merging, even though the DMC itself has vaporized.

**Table 1.** Constituents and mole fractions used in the simple surrogate models developed to simulate the behavior of the distillation curves of diesel fuel with DMC.

| Compound | Mole fraction composition of the 10 vol.-% DMC mixture | Mole fraction composition of the 20 vol.-% DMC mixture | Mole fraction composition of the 30 vol.-% DMC mixture |
|---|---|---|---|
| *n*-Nonane | 0.0200 | 0.0160 | 0.0140 |
| *n*-Decane | 0.0400 | 0.0310 | 0.0280 |
| *n*-Undecane | 0.1000 | 0.0790 | 0.0700 |
| *n*-Dodecane | 0.4046 | 0.3178 | 0.2848 |
| *n*-Tridecane | 0.1000 | 0.0790 | 0.0700 |
| *n*-Tetradecane | 0.0400 | 0.0310 | 0.0280 |
| *n*-Pentadecane | 0.0400 | 0.0310 | 0.0280 |
| *n*-Hexadecane | 0.0200 | 0.0160 | 0.0140 |
| DMC | 0.2354 | 0.3992 | 0.5368 |

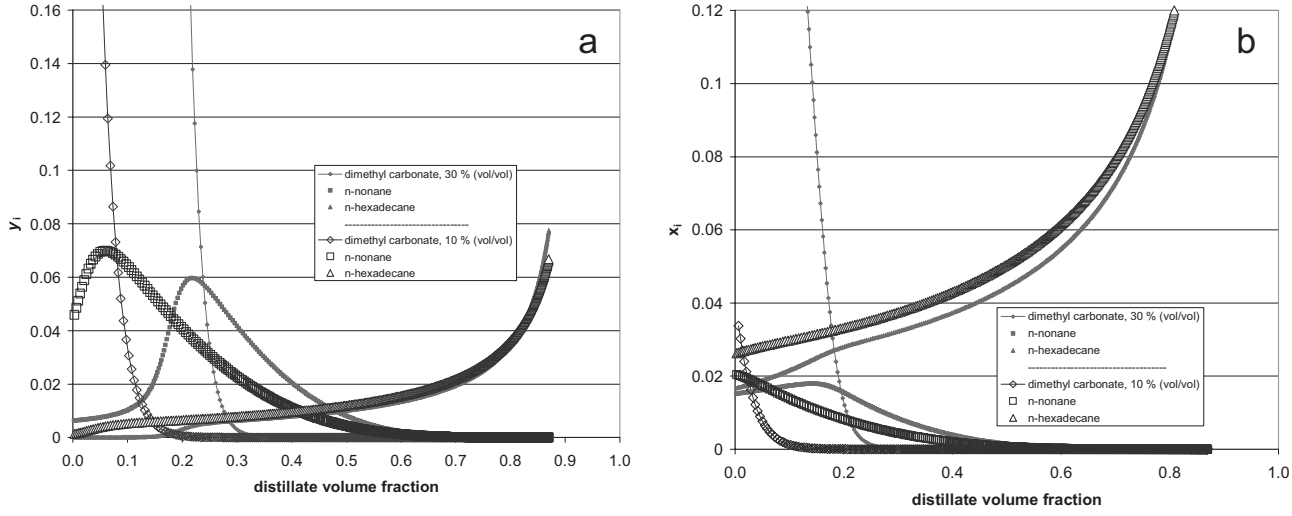


**Figure 12.** (a) Calculated distillation curves (expressed as mole fractions of vapor, $y_i$) for the mixture of 30 and 10 vol.-% DMC in the surrogate summarized in Tab. 1. (b) Calculated distillation curves (expressed as mole fractions of liquid, $x_i$) for the surrogate.

  

## 4 Conclusions

In this review, we have discussed the salient features of the composition-explicit or ADC approach for the measurement of complex, multicomponent fluids. The method bridges the gap between a chemical analysis protocol and a thermophysical property measurement in a relational manner. Thus, analytical information can be used to enhance a measure of fluid volatility, and vice versa. The result is a powerful method that can be used to characterize fluids and in the development of thermophysical property models.

*The authors have declared no conflict of interest.*

## References


[1] G. C. Klein, Dissertation submitted in partial fulfillment of the Ph.D., Department of Chemistry and Biochemistry, Florida State University, Tallahassee **2005**.
[2] A. G. Marshall, R. P. Rodgers, *Acc. Chem. Res.* **2004**, *37*, 53.
[3] O. C. Mullins, E. Y. Sheu, M. Hammadi, A. G. Marshall, *Asphaltenes, Heavy Oils, and Petroleomics*, Springer Science + Business Media, New York **2007**.
[4] H. Z. Kister, *Distillation Operation*, McGraw-Hill, New York **1988**.
[5] H. Z. Kister, *Distillation Design*, McGraw-Hill, New York **1991**.
[6] *ASTM Standard D 86-04b, Standard Test Method for Distillation of Petroleum Products at Atmospheric Pressure*, ASTM International, West Conshohocken **2004**.
[7] T. J. Bruno, *Ind. Eng. Chem. Res.* **2006**, *45*, 4371.
[8] T. J. Bruno, *Sep. Sci. Technol.* **2006**, *41 (2)*, 309.
[9] T. J. Bruno, P. D. N. Svoronos, *CRC Handbook of Basic Tables for Chemical Analysis*, 2nd ed., Taylor and Francis CRC Press, Boca Raton **2004**.
[10] T. J. Bruno, P. D. N. Svoronos, *CRC Handbook of Fundamental Spectroscopic Correlation Charts*, Taylor and Francis CRC Press, Boca Raton **2005**.
[11] M. L. Huber, B. L. Smith, L. S. Ott, T. J. Bruno, *Energy Fuels* **2008**, *22*, 1104.
[12] M. L. Huber, E. Lemmon, L. S. Ott, T. J. Bruno, *Energy Fuels* **2009**, *23*, 3083.
[13] M. L. Huber, E. W. Lemmon, V. Diky, B. L. Smith, T. J. Bruno, *Energy Fuels* **2008**, *22*, 3249.
[14] T. J. Bruno, L. S. Ott, B. L. Smith, T. M. Lovestead, *Anal. Chem.*, in press.
[15] T. J. Bruno, L. S. Ott, T. M. Lovestead, M. L. Huber, *J. Chromatogr.*, in press.
[16] B. L. Smith, T. J. Bruno, *Int. J. Thermophys.* **2006**, *27*, 1419.
[17] T. J. Bruno, *Anal. Chem.* **1986**, *58 (7)*, 1595.
[18] T. J. Bruno, in *Process Control and Quality* (Ed: E. H. Baughman), Vol. 3, Elsevier, Amsterdam **1992**.
[19] L. S. Ott, B. L. Smith, T. J. Bruno, *J. Chem. Thermodyn.* **2008**, *40*, 1352.
[20] S. Young, *Proc. Chem. Soc.* **1902**, *81*, 777.
[21] S. Young, *Fractional Distillation*, Macmillan and Co., London **1903**.
[22] S. Young, *Distillation Principles and Processes*, Macmillan and Co., London **1922**.
[23] T. J. Bruno, B. L. Smith, *Energy Fuels* **2006**, *20*, 2109.
[24] L. S. Ott, T. J. Bruno, *Energy Fuels* **2007**, *21*, 2778.
[25] L. S. Ott, T. J. Bruno, *J. Sulfur Chem.* **2007**, *28 (5)*, 493.
[26] L. S. Ott, B. L. Smith, T. J. Bruno, *Fuel* **2008**, *87*, 3055.
[27] L. S. Ott, B. L. Smith, T. J. Bruno, *Fuel* **2008**, *87*, 3379.
[28] Purchase Description, RP-1, Federal Business Opportunities, http://fs2.eps.gov/EPSData/DLA/Synopses/12671/SP0600-03-R-0322/rp-1sol.pdf, **2003**.
[29] T. J. Bruno, B. L. Smith, *Ind. Eng. Chem. Res.* **2006**, *45*, 4381.
[30] L. S. Ott, A. Hadler, T. J. Bruno, *Ind. Eng. Chem. Res.* **2008**, *47 (23)*, 9225.
[31] E. J. Buchanan, *Sugar J.* **2002**, *65 (6)*, 11.
[32] C. R. Soccol, L. P. S. Vandenburgehe, B. Costa, A. L. Woiciechoski, J. C. Carvalho, A. B. P. Medeiros, A. M. Francisco, L. J. Bonomi, *J. Sci. Ind. Res.* **2005**, *64 (11)*, 897.
[33] T. J. Bruno, A. Wolk, A. Naydich, *Energy Fuels* **2009**, *23 (6)*, 3277.
[34] F. Seemann, *Int. Sugar J.* **2003**, *105 (1257)*, 421.
[35] U. C. Upadhiya, Production of ethanol from sugarcane, in *Iberia Sugar TEC-254*, Iberia Sugar, Florida **1996**.
[36] B. D. Yaccobucci, Fuel ethanol: Background and public policy issues, *CRS Report for Congress, RL33290*, Congressional Research Service, Washington, D.C., March 3, **2006**.
[37] T. M. Lovestead, T. J. Bruno, *Energy Fuels* **2009**, *23 (7)*, 3637.
[38] B. L. Smith, T. J. Bruno, *Ind. Eng. Chem. Res.* **2007**, *46*, 297.
[39] B. L. Smith, T. J. Bruno, *Ind. Eng. Chem. Res.* **2007**, *46*, 310.
[40] B. L. Smith, T. J. Bruno, *J. Propul. Power* **2008**, *24 (3)*, 619.
[41] T. J. Bruno, A. Wolk, A. Naydich, *Energy Fuels* **2009**, *23*, 2295.
[42] L. S. Ott, B. L. Smith, T. J. Bruno, *Energy Fuels* **2008**, *22*, 2518.
[43] B. L. Smith, L. S. Ott, T. J. Bruno, *Environ. Sci. Technol.* **2008**, *42 (20)*, 7682.
[44] T. J. Bruno, A. Wolk, A. Naydich, M. L. Huber, *Energy Fuels* **2009**, *23 (8)*, 3989.
[45] T. M. Lovestead, T. J. Bruno, *Energy Fuels* **2009**, *23*, 2176.
[46] A. B. Hadler, L. S. Ott, T. J. Bruno, *Fluid Phase Equilib.* **2009**, *281*, 49.
[47] T. J. Bruno, A. Wolk, A. Naydich, *Energy Fuels* **2009**, *23*, 1015.
[48] L. S. Ott, T. J. Bruno, *Energy Fuels* **2008**, *22*, 2861.
[49] J. A. Widegren, T. J. Bruno, *Energy Fuels* **2008**, in press.
[50] J. A. Widegren, T. J. Bruno, *Proc. 4th Liquid Propulsion Subcommittee, JANNAF*, Orlando **2008**.
[51] E. W. Lemmon, M. O. McLinden, M. L. Huber, *REFPROP, Reference Fluid Thermodynamic and Transport Properties, NIST Standard Reference Database 23*, National Institute of Standards and Technology, Gaithersburg **2005**.
[52] E. W. Lemmon, R. T. Jacobsen, *J. Phys. Chem. Ref. Data* **2004**, *33 (2)*, 593.
[53] B. L. Smith, T. J. Bruno, *Energy Fuels* **2007**, *21*, 2853.


  